The International Archives of the Photogrammetry, Remote Sensing and Spatial Information Sciences, Volume XLVIII-4/W1-2022
Free and Open Source Software for Geospatial (FOSS4G) 2022 – Academic Track, 22–28 August 2022, Florence, Italy

MONITORING LANDSLIDE DISPLACEMENTS THROUGH MAXIMUM CROSS-CORRELATION OF SATELLITE IMAGES

Lorenzo Amici[1,*], Vasil Yordanov[1,2], Daniele Oxoli[1], Xuan Quang Truong[3], Maria Antonia Brovelli[1,4]

[1]Department of Civil and Environmental Engineering (DICA), Politecnico di Milano, Piazza Leonardo da Vinci 32, Milan, Italy (lorenzo.amici, vasil.yordanov, daniele.oxoli, maria.brovelli)@polimi.it
[2]Vasil Levski National Military University, Veliko Tarnovo, Bulgaria - vasil.yordanov@polimi.it
[3]Hanoi University of Natural Resources and Environment, 41A Phu Dien Road, Phu Dien, North-Tu Liem district, Hanoi txquang@hunre.edu.vn
[4]Istituto per il Rilevamento Elettromagnetico dell'Ambiente, CNR-IREA, via Bassini 15, 20133 Milano - maria.brovelli@polimi.it

Commission IV, WG IV/4

KEY WORDS: Landslide displacement monitoring, Earth Observation, Maximum Cross-Correlation, satellite images

ABSTRACT:

Landslides are one of the most dangerous and disastrous geological hazard worldwide, posing threats to human life, infrastructures and to the natural environment. Consequently, monitoring active landslides is crucial in order to reduce the risk of damages and casualties. With this aim, this work proposes a way to compute landslide displacements through time, by exploiting the great availability of high quality multispectral satellite images. The developed procedure produces maps of displacement magnitude and direction by means of local cross-correlation of Earth Observation data from the Sentinel-2 and PlanetScope missions. The Ruinon landslide, an active landslide in Northern Lombardy, Italy, was selected as a case study. The workflow of the developed procedure is described, and the results are presented and discussed. Moreover, a validation of the analysis by comparison with UAV surveys of the landslide is reported, along with a discussion on future developments and improvements of this technique. This work was designed to be entirely based on free and open-source GIS software and to rely mainly on open data. These characteristics allow the proposed analysis to be easily replicated, customized, and empowered.

1. INTRODUCTION

Landslides are a widespread geological hazard which often deals serious damages to the environment and to anthropogenic infrastructures, while also causing economic losses and casualties (Guzzetti et al., 2012). It has also been shown that the population growth and the consequent expansion of settlements of the last decades are magnifying the impact of such phenomena (Guzzetti et al., 2012). Moreover, we are also witnessing a rise in the extreme events that trigger landslides, as a consequence of climate change (Machichi et al., 2020).

In particular, Italy is extremely affected by landslides, specifically due to the geological and morphological characteristics of the Italian territory, that consists for the main part of mountains and hills. Indeed, Italy is the European country most affected by landslides, and as of 2015, 2/3 of the landslides recorded in Europe took place in Italy.

The growth of the availability of free and open multispectral, multitemporal and global coverage satellite imagery plays an integral role in studies focusing on detecting changes in the surface of the Earth. By taking advantage of such images, scholars have indeed carried out analyses with the intent of monitoring various phenomena on Earth's surface, such as glacier movement (Berthier et al., 2005), land cover changes (Dewan and Yamaguchi, 2009) and forest growth or deforestation (Coppin and Bauer, 1996; Kennedy et al., 2010). Making archive data and newly sensed images available with an open distribution policy has also promoted the growth of the user community and the development of applications in order to take advantage of such data (Oxoli et al., 2020). A notable example of the above are the ESA Sentinel missions (ESA, 2022), which played a fundamental role in the outlining of this work.

* Corresponding author

In view of the above, monitoring active landslides is crucial when trying to mitigate the risk posed by these phenomena. Hence, this work proposes a procedure for computing landslide displacements through time by means of a cross-correlation of multispectral satellite images (Amici et al., 2022). This experimental procedure was developed with the goal of receiving as input an Earth Observation data stack and returning as output pixel-level displacement maps; the output maps highlight both the displacement magnitude and the displacement direction, therefore identifying a *displacement vector*.

The procedure was developed using solely Geographic Information Systems (GIS) Free and Open Source Software (FOSS), and it was tested over a single landslide in Italy (Ruinon landslide) using both Sentinel-2 and PlanetScope images (Planet Team, 2022a). Details about the data and the area of interest can be found in Section 2, while Section 3 illustrates the methodology of the workflow. The obtained results are presented in Section 4, and Section 5 outlines the conclusions and future improvements of this work.

2. AREA OF INTEREST AND DATA

2.1 Landslide of interest

The developed procedure was tested on the Ruinon landslide, situated in Northern Lombardy, Italy. This particular landslide was chosen for a series of reasons: first, its monitoring is of great relevance, since it is one of the most active landslides in the Alps; secondly, it has been particularly active in the last years, facilitating the use of Sentinel-2 and PlanetScope satellite images; and finally, its extension, movement typology and velocity are optimal for the chosen analytical method. The Ruinon landslide is situated at the base of a Deep-seated Gravitational Slope Deformation, that affects the entire slope up to the summit at 3000 m a.s.l. The landslide is believed to extend down to a depth of 50–70 m, for a total estimated volume of approximately 30 million m^3. Furthermore, it can be subdivided in two scarps: the upper one is a sub-vertical rock cliff of about 30 m in height, while the lower one is characterized by a more widespread debris cover (Figure 1). Over the years, a large lobe of chaotic debris has propagated towards the valley bottom, giving origin to secondary mass wasting processes in the form of rockfalls, debris flows, and shallow slumps (Carlà et al., 2021).

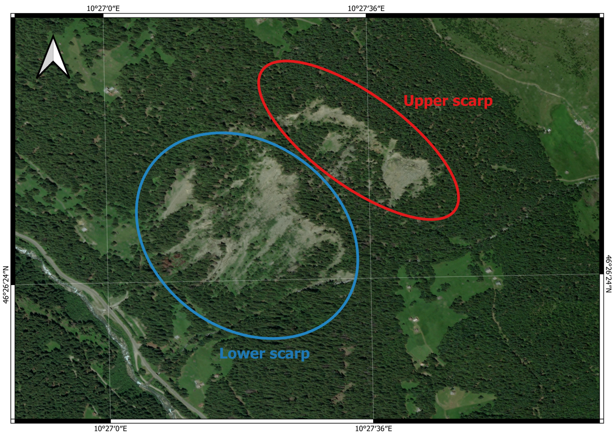

Figure 1. Ruinon landslide © Esri World Imagery, Source: Esri, Maxar, Earthstar Geographics, and the GIS User Community

2.2 Satellite data

The developed software is intended to work with multispectral satellite images taken on the same area at different times. This characteristic entails that the area to be considered must not be covered by clouds, and that the terrain must be free from snow. To achieve such results, the EO browsers for both Sentinel-2 and PlanetScope data were used to carefully inspect images over the chosen Area Of Interest (AOI) and select the ones to be downloaded.

2.2.1 Sentinel-2: Images collected by the Sentinel-2 satellites were downloaded through the official portal of the Copernicus programme, the Copernicus Open Access Hub (Copernicus Programme, 2022). For this analysis, Top-of-atmosphere Sentinel-2 Level-1C products were considered (Figure 2). In the case of Sentinel data, the images were used for two different purposes: an analysis of the activity of the landslide over the last years, by selecting one image per year from 2015 to 2020, and a focus on the summer months of 2019, which was a period of intense activity for the Ruinon landslide. The downloaded data are summarized in Table 1.

2.2.2 PlanetScope: Planet is a company that provides commercial daily satellite data to businesses, governments and journalists (Planet Team, 2022b). They also provide limited, non-commercial access to PlanetScope and RapidEye imagery to researchers and students as part of their Education and Research Program. PlanetScope images were considered in the

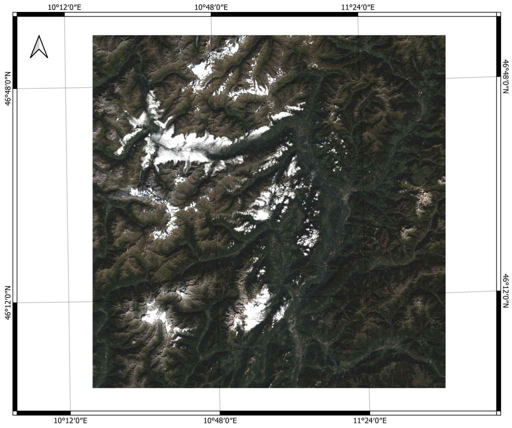

Figure 2. Example of one of the downloaded Sentinel-2 Level-1C tiles, in True Colours visualization

Mission	Date	Used for		
		Y	S	V
S2A	08/03/2015	✓		
S2A	08/27/2016	✓		
S2A	07/09/2017	✓		
S2A	07/08/2018	✓		
S2A	07/23/2019		✓	
S2B	08/27/2019	✓	✓	
S2A	09/21/2019		✓	✓
S2A	08/26/2020	✓		
S2A	09/15/2020			✓

Table 1. Downloaded Sentinel-2 images and their application in this work (Y = yearly analysis, S = summer 2019 analysis, V = validation)

context of this work because they have a resolution of 3 m, higher than the Sentinel-2 one, and thus could provide more accurate insights about the movement of the landslide. In particular, the analyses done with Sentinel-2 data were replicated with PlanetScope images, thus enabling a comparison between different data choices. The downloaded data are summarized in Table 2.

Date	Used for	
	Y	S
08/22/2016	✓	
07/07/2017	✓	
07/13/2018	✓	
07/10/2019		✓
07/23/2019		✓
07/24/2019	✓	
09/21/2019		✓
08/27/2020	✓	

Table 2. Downloaded PlanetScope images and their application in this work (Y = yearly analysis, S = summer 2019 analysis)

3. LANDSLIDE DISPLACEMENT ANALYSIS

3.1 Tools and technologies

The general strategy employed in this work for obtaining landslide displacements in terms of direction and magnitude is to apply a local Maximum Cross-Correlation (MCC) analysis on a multitemporal images stack. MCC is a method for computing pixel changes between two images; in the past this technique was mainly applied to geophysical phenomena involving fluid motion, such as the movement of clouds (Leese et al., 1971), sea (Crocker et al., 2007) or glaciers (Ninnis et al., 1986). Concerning terrestrial land-cover changes, techniques based on cross-correlation have been generally applied by comparing pixels or objects in two different images; these methods usually produce maps that indicate if a pixel value has changed or not between the two images, without being able to identify a movement vector. On the other hand, more recent studies have applied the MCC method to identify directional changes, quantifying the movement detected for every single pixel: You et al. (2017) were the first to apply the MCC method to identify and quantify the direction of land-cover changes in a river floodplain in Bolivia using Landsat-5 Thematic Mapper images, while Oxoli et al. (2020) considered Landsat-8 and Sentinel-2 satellite images to detect the movements of desert dunes using MCC.

The procedure was developed using GRASS GIS (OSGeo, 2022) and custom Python scripts. The reasoning behind the preference of GRASS GIS among other GIS applications was mainly the high synergy between GRASS and Python programming, that allows to combine in a single Python script the functionalities and image processing capabilities offered by GRASS functions with the power and flexibility of the Python programming language. In particular, a set of scripts was developed in order to carry out each of the processing steps, which are illustrated in the next sections, in a standalone way.

3.2 Workflow

The process (Figure 3) starts with the download of the images and the creation of a suitable images stack, ordered by ascending date of acquisition, that represent the input of the analysis. After the preprocessing, which is carried out on each image independently from the others, the procedure iteratively considers couples of images acquired at different times t and $t + \Delta t$: when this is the case, the image taken at time t will be referred to as *reference image*, while the image successively taken at time $t + \Delta t$ will be referred to as *secondary image*. In this work, two methods are considered for establishing the *reference/secondary* relationship:

- Fixed *reference*, i.e. the *reference* is fixed to the first chronological image and all the other images are coupled with it;
- Moving *reference*, i.e. the *reference* is always the previous chronological image with respect to the *secondary* one.

3.2.1 Preprocessing: Preprocessing steps are applied to the downloaded satellite imagery with the aim to produce a suitable multitemporal stack. The preprocessing procedure is composed of three main operations: cloud masking, atmospheric correction in the form of Dark Object Subtraction (DOS), and the creation of a single multiband output raster by combining the preprocessed bands. It is important to note that for Sentinel images not all the bands are preprocessed; in particular, the 60 m original resolution bands, i.e. aerosol (band 1), water vapour (band 9), and cirrus (band 10) are excluded. For PlanetScope on the other hand, the Red, Green, Blue and NIR bands are considered for the whole process.

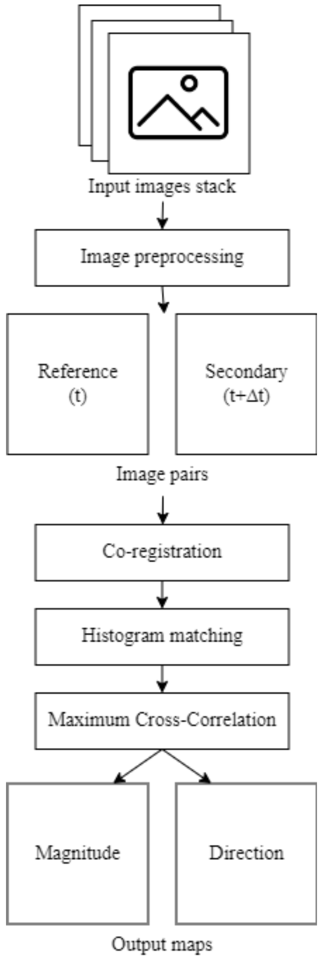

Figure 3. Schematic of the proposed workflow for landslide displacement analysis using multispectral data

3.2.2 Co-registration: This step is crucial in analyses like the one outlined in this work, in order to ensure that the images become spatially aligned so that any feature in one image overlaps as well as possible its footprint in all other images in the stack. Some small misalignments, in the range from sub-pixel to few pixels, can occur when images from different sensors are used, but in some cases also between images with the same sensor. In the case of the Sentinel-2 images the AROSICS (Automated and Robust Open-Source Image Co-Registration Software) package (Scheffler et al., 2017) was used. The approach is based on phase correlation to detect local/global shifts at sub-pixel level. On the other hand, for the co-registration step of the PlanetScope imagery the GeFolki package (Brigot et al., 2016) was used, which is an optical-flow estimation technique based on Lucas-Kanade approach and optimization of the eFolki (Plyer et al., 2015) approach for heterogeneous image co-registration. Using the GeFolki algorithms has some advantages that are producing more robust image alignment – the approach is working on an iterative local neighbourhood principle but is also a multi-resolution, by adopting a pyramid scheme for the images in a coarse-to-fine strategy (Plyer et al., 2015), which allows to determine larger displacements despite the local limitations. In addition, GeFolki adopts two filtering steps that are dealing with matching image textures (Rolling Guidance Filter) and contrast difference between two images (Local Contrast Inversion). The co-registration for both of the datasets (Sentinel-2 and PlanetScope) was following the previously mentioned fixed/moving reference-secondary scheme.

3.2.3 Histogram matching: The images' histograms are matched, thus transforming the cumulative distribution function (CDF) of values in each band of an image in order to match the CDF of the corresponding bands in another image, for the sake of improving comparability between the data. This operation is carried out using the dedicated function of the *scikit-image* Python library.

3.2.4 Processing: The displacement detection analysis takes into consideration a couple of images at the time, and applies the Maximum Cross-Correlation method to the two scenes. The algorithm starts by defining a window of the same size and in the same position for both images. The window on the *secondary image* is then shifted in all directions (Figure 4(b)), and a cross-correlation coefficient (ρ) is computed considering each of the shifted windows and the *reference* window. The position of the shifted window that maximizes the cross-correlation coefficient is selected, and the direction and length of the displacement (i.e. of the shift) are computed and saved in output files. The algorithm then proceeds to center the moving window on another pixel and the whole process is repeated for each pixel of the images. The cross-correlation computation is performed using the *phase_cross_correlation* function of the *scikit-image* Python library, which outputs the X and Y shifts (in pixels) required to register two scenes. The cross-correlation coefficient can be computed using the following formula:

$$\rho(i,j) = \frac{cov[A(x_r,y_r),B(x_s,y_s)]}{\sqrt{var[A(x_r,y_r)]var[B(x_s,y_s)]}} \tag{1}$$

where the subscript *r* indicates the *reference image* and the subscript *s* the *secondary image*. Therefore, $A(x_r, y_r)$ is the set of pixels of the *reference image* inside the window centred in (x_r, y_r), while $B(x_s, y_s)$ is the set of pixels of the *secondary image* inside the window centred in (x_s, y_s), i.e. in $(x_r + i, y_r + j)$.

3.3 Limitations

The developed procedure is able to identify magnitude and direction of landslide displacements at pixel level, but it suffers from two main limitations. Firstly, the minimum displacement between two images that can be identified by this analysis is a displacement of 1 pixel, i.e. a displacement of 10 m for the case of Sentinel-2 and of 3 m for PlanetScope. Smaller movements cannot be sensed by this procedure because of the native resolution of input satellite data, and this entails that the procedure is not suited for monitoring both smaller and slower mass movements. Secondly, the procedure is highly influenced by errors in terms of co-registration and histogram matching of the images, since the whole process relies on the scenes to be as aligned and similar as possible. The issue related to the pixel value differences (i.e. colour differences) could be solved by applying an unsupervised classification to each scene in order to distinguish *landslide* pixels from *no landslide* ones; this approach was explored but eventually not included in the procedure since along the landslide body the trees and the bare soil usually merge and the classification struggles to consistently classify them.

4. RESULTS

As stated before, in this work we chose to compute the displacements of the Ruinon landslide in two different time intervals.

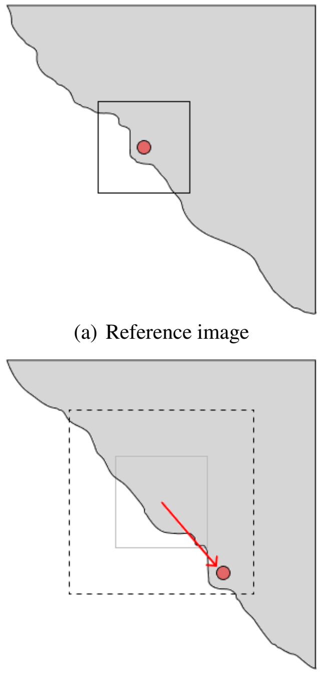

(a) Reference image

(b) Secondary image

Figure 4. Illustration of the Maximum Cross-Correlation algorithm

Firstly, an analysis of the movement over the last years was carried out, considering one image per year from 2015 to 2020; since several mass movements originated on the surface of the landslide in this period, it was considered of interest to inspect the evolution of the landslide year by year. Secondly, since a large debris slide was documented between July and August 2019, we decided to apply the procedure to that period.

4.1 Output maps

Figure 5 and Figure 6 illustrate an example of the output maps obtained from the procedure. Both figures depict the reference and secondary maps, from 2019 and 2020, and the resulting features of the displacements computed between those dates. The shown examples are computed with moving windows of sizes 7x7 pixels for Sentinel-2 and 21x21 pixels for PlanetScope data.

4.2 Result synthesis

The procedure outputs two maps, one for the displacement magnitude and one for its direction, for each pair of images analysed. This feature can be disadvantageous if the objective is to globally investigate landslide movements in a given period, since the maps only display movements between two epochs. Thus, a strategy for summarizing the results was in need, and windrose diagrams were considered and eventually chosen to achieve result synthesis. A windrose diagram allows to plot the obtained displacements as oriented histograms, therefore simultaneously giving information about the direction of the movement, the quantity (percentage) of pixels moving in that direction and the magnitude of the displacements. In addition, for producing the windroses only pixels that had a cross-correlation error smaller than an arbitrary threshold were considered, therefore filtering out bad results. Windrose diagrams were therefore generated for both the fixed and moving reference approach and for each of the analysis periods using the *windrose* Python library (Roubeyrie and Celles, 2018); the results for the yearly

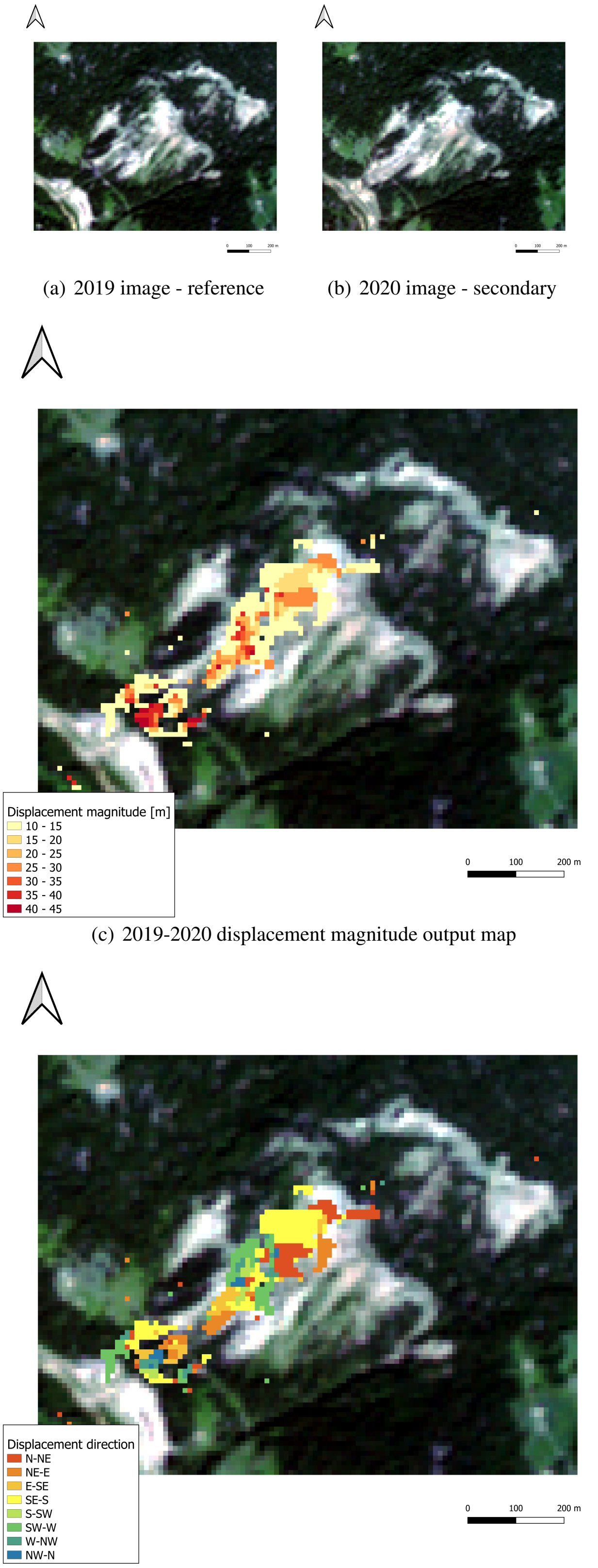

(a) 2019 image - reference (b) 2020 image - secondary

(c) 2019-2020 displacement magnitude output map

(d) 2019-2020 displacement direction output map

Figure 5. Sentinel-2 input and output maps for the analysis between 2019 and 2020

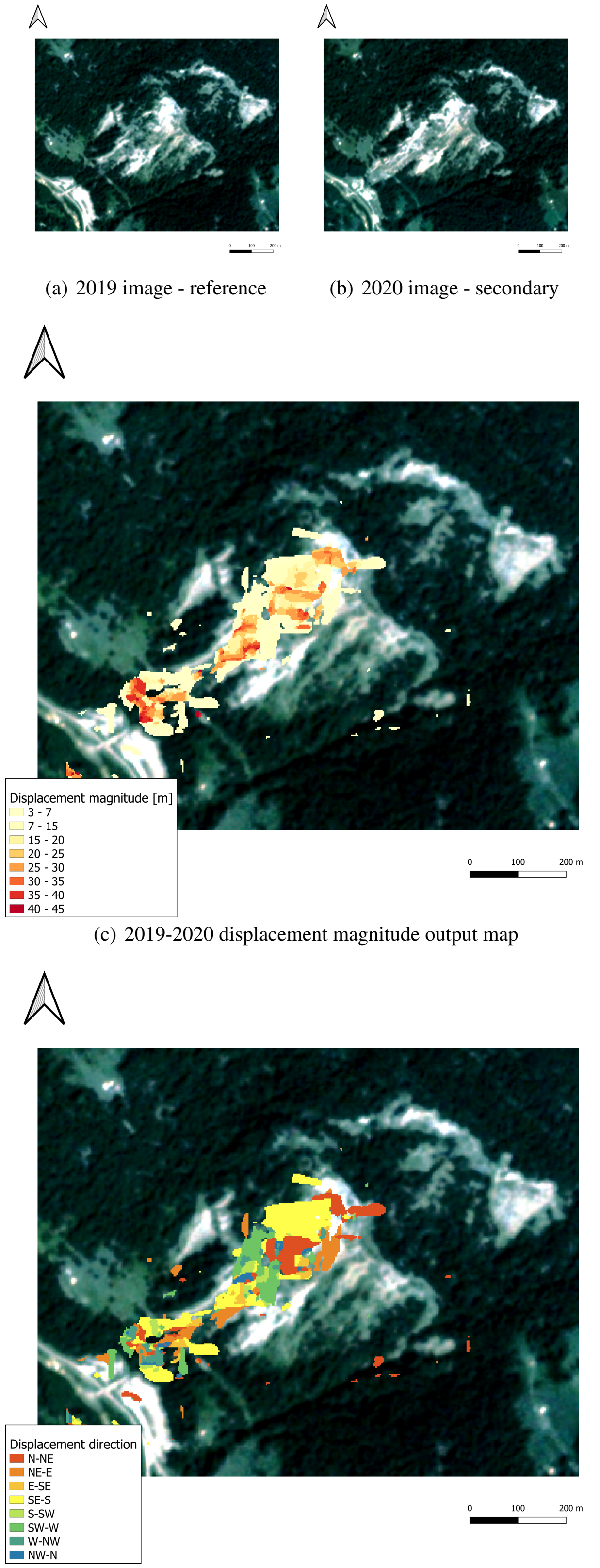

(a) 2019 image - reference (b) 2020 image - secondary

(c) 2019-2020 displacement magnitude output map

(d) 2019-2020 displacement direction output map

Figure 6. PlanetScope input and output maps for the analysis between 2019 and 2020

analysis are reported in Figure 7 and Figure 8. From the windrose diagrams, we can see that the majority of moving pixels is sliding towards South; this is partially consistent with the real movement, even though in reality the Ruinon landslide is mostly moving along the South-West diagonal. On the other hand, by comparing the windroses obtained with different data sources, their agreement is an indicator of the validity of this technique.

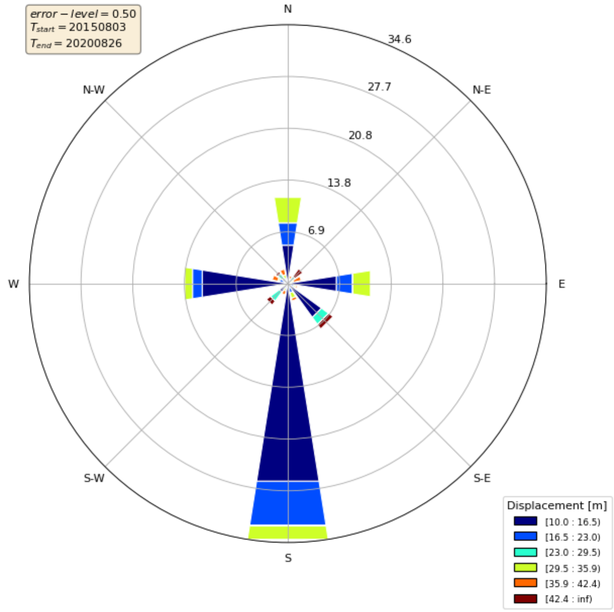

Figure 7. Windrose for Sentinel-2 data yearly analysis with *moving reference* approach

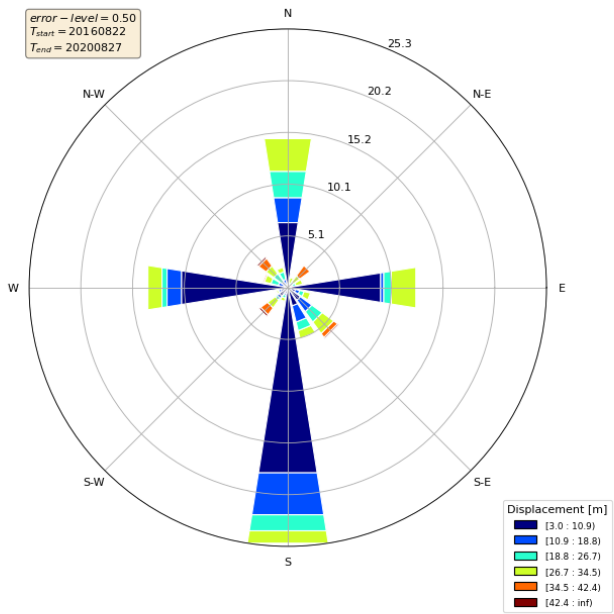

Figure 8. Windrose for PlanetScope data yearly analysis with *moving reference* approach

4.3 Result comparison

As shown by Figure 5 and Figure 6, the output obtained by cross-correlating Sentinel-2 images is very similar to the one obtained with PlanetScope data. The same portions of the landslide are identified as moving, and the displacements are comparable in terms of both their magnitude and direction. Due to the higher resolution, PlanetScope data allow the procedure to identify displacements in the range 3-10 m, which is not possible using Sentinel-2 images. On the other hand, the higher resolution of PlanetScope images is probably the cause for a greater quantity of noise around the landslide; Figure 9 is an example of this issue, since some of the vegetation pixels around the landslide body are identified as moving, probably because Planet satellites generate more detailed images and therefore changes in the vegetation or illumination of the zone become clearer, and the procedure becomes susceptible to these kinds of misinterpretation. This problem is also evident by considering the windrose diagrams; the one for PlanetScope data (Figure 8) shows a higher quantity of pixels moving towards North, which in the case of the Ruinon landslide is considered an error since the landslide moves towards the South-West direction.

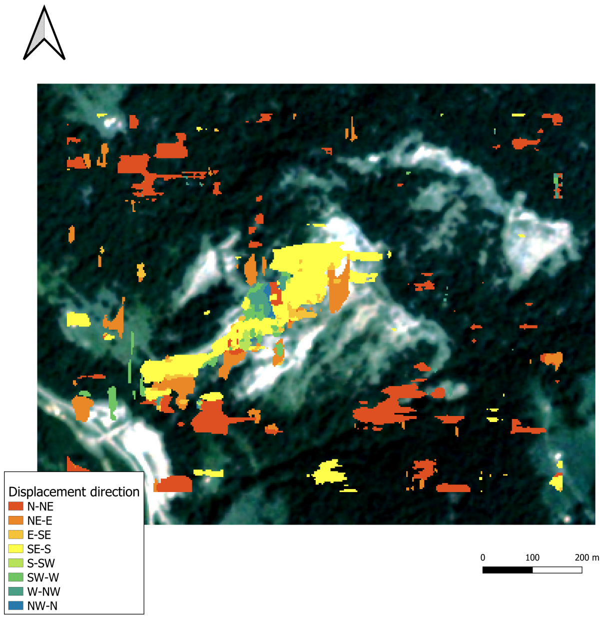

Figure 9. Cross-correlation of PlanetScope images and noise around the landslide

4.4 Validation

Due to its recent activity, the Ruinon landslide has been monitored with UAV surveys by ARPA Lombardia (the regional agency for environmental protection) from 2019 to 2020, and by the GEOLab of Politecnico di Milano, from 2021 onwards (Yordanov et al., 2022). The data collected in these surveys were made available and were used for validating the procedure developed in this work. The procedure was validated considering the results obtained with Sentinel-2 data, given the free and open availability of Sentinel images. In particular two recent ARPA surveys (one in 2019 and one in 2020) were selected for the validation, and two Sentinel images sensed in the same periods were downloaded. The displacement monitoring procedure was applied to both the Sentinel-2 images (Figure 10(a)) and the RGB images from the surveys resampled to a resolution of 10 m (Figure 10(b)), and the obtained results were compared. Overall the two outputs depict the same portions of the body of the landslide as moving; moreover, also the values of the displacements are similar between the two analyses, given that the mean value of the differences between the magnitude output rasters is of 5 m and the mean value of the differences between the direction output rasters is of -18°.

For further validation, the displacements along the Z axis, obtained from the UAV surveys, were inspected (Figure 11). The right flank of the body of the landslide was considered, since it corresponds to the part showing a greater movement from the

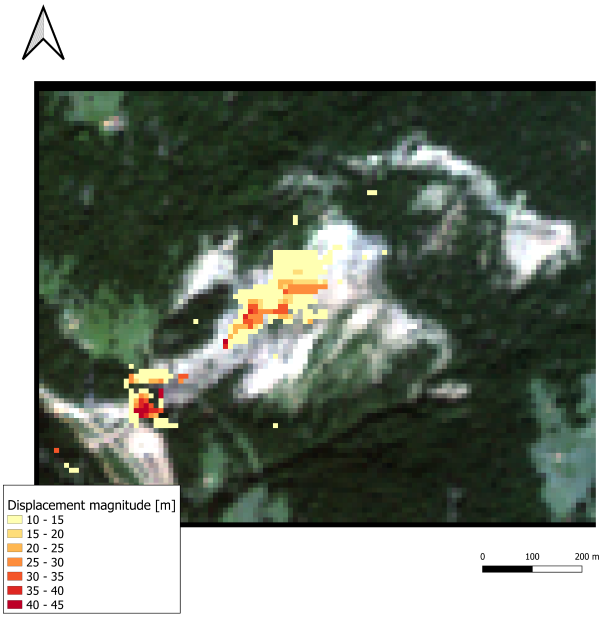

(a) Displacement magnitude output from Sentinel-2 images

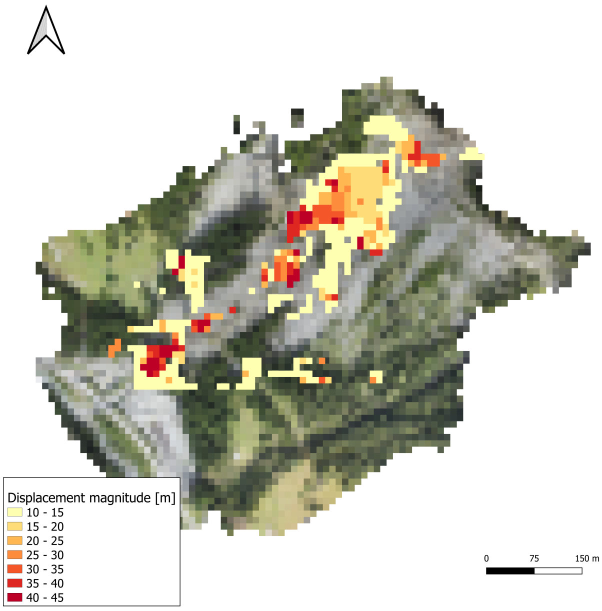

(b) Displacement magnitude output from upsampled UAV RGB images

Figure 10. Sentinel-2 and UAV outputs used for validation

outputs of Sentinel-2. It was seen that between the two surveys an accumulation zone appears in correspondence with the large movement detected by the procedure on the bottom of the right flank (Figure 12). In particular, a positive increase of the terrain Z of 4 m, due to accumulation of material, was detected by comparing the point clouds from the surveys. This was considered in accordance to the movement detected by the developed procedure, thus confirming the validity of the results.

5. CONCLUSIONS

In this paper, a semi-automatic procedure for detecting landslide displacements by means of multispectral imagery analysis through time was presented, and the results obtained by applying the procedure to a landslide in Italy were shown and commented.

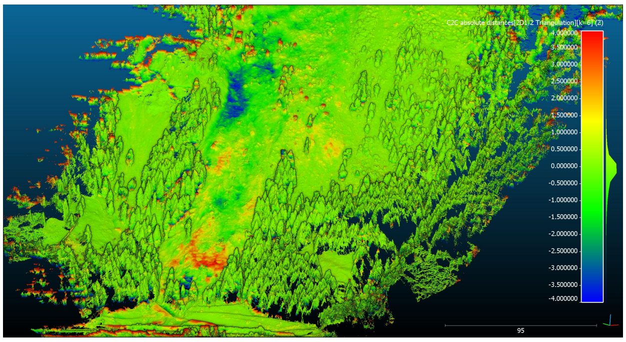

Figure 11. Differences along the Z axis between the two UAV surveys

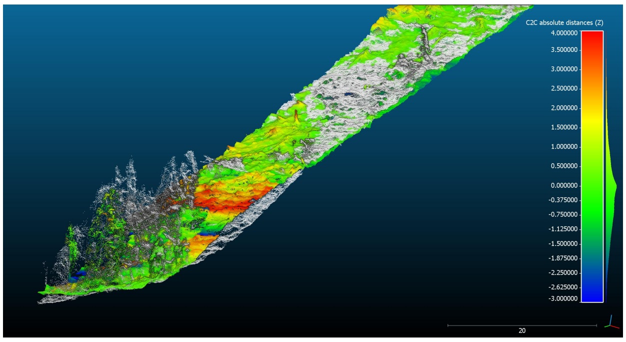

Figure 12. Differences along the Z axis between the two UAV surveys: focus on bottom part of the landslide

As already stated, the monitoring of active landslides is a matter of primary importance when dealing with mass movement phenomena, and the increased availability of high-resolution multitemporal satellite imagery promotes the use of these images for monitoring purposes. While *in situ* monitoring can produce very accurate results, a procedure like the one applied in this work has the advantage to be more flexible, scalable and cost-effective than an analysis on-site.

Despite being a first stage approach to landslide monitoring with the Maximum Cross-Correlation technique, this procedure led to promising results. The obtained results showed a partial agreement with real world data, and the procedure was applied to heterogeneous data sources with comparable results for validation. However, additional work is required, including primarily testing the performances of the procedure on landslides with different characteristics (e.g. movement type, velocity, extension, lithology etc.) than the one chosen for this work. Moreover, mitigating as much as possible the errors arising from the preprocessing phases could only benefit analyses like the one presented in this paper.

Finally, a core strength of this work is that it relies exclusively on Geographic Information Systems Free and Open Source Software (FOSS GIS). In view of the spread of landslide phenomena and of the importance of landslide monitoring, this feature allows this work to be easily replicated, adapted, improved and empowered.

ACKNOWLEDGEMENTS

The author would like to thank ARPA Lombardia, specifically Doctors Dario Bellingeri, Luca Dei Cas, Alessandro Menin and

Enrico Zini, for supporting this research with data and suggestions. The work is partially funded by the Italian Ministry of Foreign Affairs and International Cooperation within the project "Geoinformatics and Earth Observation for Landslide Monitoring" - CUP D19C21000480001 (Italian side) and partially funded by Ministry of Science and Technology of Vietnam (MOST) (Vietnamese side) by the Bilateral Scientific Research project between Vietnam and Italy, code: NĐT/IT/21/14.

References

Amici, L., Yordanov, V., Oxoli, D., Brovelli, M. A., 2022. Monitoring Landslide Displacements Through Maximum Cross-Correlation of Sentinel-2 Satellite Images. *GIS Ostrava 2022 Earth Observation for Smart City and Smart Region*.

Berthier, E., Vadon, H., Baratoux, D., Arnaud, Y., Vincent, C., Feigl, K. L., Rémy, F., Legrésy, B., 2005. Surface motion of mountain glaciers derived from satellite optical imagery. *Remote Sensing of Environment*, 95(1), 14–28.

Brigot, G., Colin-Koeniguer, E., Plyer, A., Janez, F., 2016. Adaptation and Evaluation of an Optical Flow Method Applied to Coregistration of Forest Remote Sensing Images. *IEEE Journal of Selected Topics in Applied Earth Observations and Remote Sensing*, 9(7), 2923–2939.

Carlà, T., Gigli, G., Lombardi, L., Nocentini, M., Casagli, N., 2021. Monitoring and analysis of the exceptional displacements affecting debris at the top of a highly disaggregated rockslide. *Engineering Geology*, 294.

Copernicus Programme, 2022. Copernicus Open Access Hub. `https://scihub.copernicus.eu` (01 June 2022).

Coppin, P., Bauer, M., 1996. Digital Change Detection in Forest Ecosystems with Remote Sensing Imagery. *Remote Sensing Reviews*, 13(3-4), 207–234.

Crocker, R., Matthews, D., Emery, W., Baldwin, D., 2007. Computing coastal ocean surface currents from infrared and ocean color satellite imagery. *IEEE Transactions on Geoscience and Remote Sensing*, 45(2), 435-447.

Dewan, A. M., Yamaguchi, Y., 2009. Land use and land cover change in Greater Dhaka, Bangladesh: Using remote sensing to promote sustainable urbanization. *Applied Geography*, 29(3), 390–401. http://dx.doi.org/10.1016/j.apgeog.2008.12.005.

ESA, 2022. Sentinel Missions. `https://sentinel.esa.int/web/sentinel` (01 June 2022).

Guzzetti, F., Mondini, A. C., Cardinali, M., Fiorucci, F., Santangelo, M., Chang, K. T., 2012. Landslide inventory maps: New tools for an old problem. *Earth-Science Reviews*, 112(1-2), 42–66. http://dx.doi.org/10.1016/j.earscirev.2012.02.001.

Kennedy, R. E., Yang, Z., Cohen, W. B., 2010. Detecting trends in forest disturbance and recovery using yearly Landsat time series: 1. LandTrendr - Temporal segmentation algorithms. *Remote Sensing of Environment*, 114(12), 2897–2910. http://dx.doi.org/10.1016/j.rse.2010.07.008.

Leese, J. A., Novak, C. S., Clark, B. B., 1971. Automated technique for obtaining cloud motion from geosynchronous satellite data using cross correlation. *Journal of Applied Meteorology*, 10(1), 118-132.

Machichi, M., Saadane, A., Guth, P., 2020. On the viability of Neural Networks for landslide susceptibility mapping in the Rif, North of Morocco. *Proceedings - 2020 IEEE International Conference of Moroccan Geomatics, MORGEO 2020*.

Ninnis, R. M., Emery, W. J., Collins, M. J., 1986. Automated extraction of pack ice motion from advanced very high resolution radiometer imagery. *Journal of Geophysical Research: Oceans*, 91(C9), 10725-10734.

OSGeo, 2022. GRASS GIS. `https://grass.osgeo.org/` (25 May 2022).

Oxoli, D., Brovelli, M. A., Frizzi, D., Martinati, S., 2020. Detection of land cover displacements through time-series analysis of multispectral satellite imagery: Application to desert. *International Archives of the Photogrammetry, Remote Sensing and Spatial Information Sciences - ISPRS Archives*, 43(B3), 739–744.

Planet Team, 2022a. Planet Application Program Interface: In Space for Life on Earth. `https://api.planet.com` (02 May 2022).

Planet Team, 2022b. PlanetScope Real-time satellite monitoring. `https://www.planet.com/products/monitoring/` (01 June 2022).

Plyer, A., Colin-Koeniguer, E., Weissgerber, F., 2015. A New Coregistration Algorithm for Recent Applications on Urban SAR Images. *IEEE Geoscience and Remote Sensing Letters*, 12(11), 2198–2202.

Roubeyrie, L., Celles, S., 2018. Windrose: A Python Matplotlib, Numpy library to manage wind and pollution data, draw windrose. *Journal of Open Source Software*, 3(29), 268.

Scheffler, D., Hollstein, A., Diedrich, H., Segl, K., Hostert, P., 2017. AROSICS: An automated and robust open-source image co-registration software for multi-sensor satellite data. *Remote Sensing*, 9(7).

Yordanov, V., Biagi, L., Truong, X. Q., Brovelli, M. A., 2022. Landslide surveys using low-cost UAV and FOSS photogrammetric workflow. *The International Archives of the Photogrammetry, Remote Sensing and Spatial Information Sciences*, XLIII-B2-2022, 493–499.

You, M., Filippi, A. M., Güneralp, I., Güneralp, B., 2017. What is the direction of land change? A new approach to land-change analysis. *Remote Sensing*, 9(8), 1–18.